Quarterly Progress Report

N01-NS-1-2333

Restoration of Hand and Arm Function by Functional Neuromuscular Stimulation

Period covered: July 1, 2002 to September 30, 2002

Principal Investigator: Robert F. Kirsch, Ph.D.

Co-Investigators:

Patrick E. Crago, Ph.D.
P. Hunter Peckham, Ph.D.
Warren M. Grill, Ph.D.
J. Thomas Mortimer, Ph.D.
Kevin L. Kilgore, Ph.D.
Michael W. Keith, M.D.
David L. Wilson, Ph.D.
Dawn Taylor, Ph.D.
Joseph M. Mansour, Ph.D.
Jeffrey L. Duerk, Ph.D.
Wyatt S. Newman, Ph.D.
Harry Hoyen, M.D.
John Chae, M.D.
Jonathon S. Lewin, M.D.
Dustin Tyler, Ph.D.

Program Manager: William D. Memberg, M.S.

Case Western Reserve University
Wickenden 407
10900 Euclid Avenue
Cleveland, OH 44106-7207
216-368-3158 (voice)
216-368-4969 (FAX)
rfk3@po.cwru.edu

Contract abstract

The overall goal of this contract is to provide virtually all individuals with a cervical level spinal cord injury, regardless of injury level and extent, with the opportunity to gain additional useful function through the use of FNS and complementary surgical techniques. Specifically, we will expand our applications to include individuals with high tetraplegia (C1-C4), low tetraplegia (C7), and incomplete injuries. We will also extend and enhance the performance provided to the existing C5-C6 group by using improved electrode technology for some muscles and by combining several upper extremity functions into a single neuroprosthesis. The new technologies that we will develop and implement in this proposal are: the use of nerve cuffs for complete activation in high tetraplegia, the use of current steering in nerve cuffs, imaging-based assessment of maximum muscle forces, denervation, and volume activated by electrodes, multiple DOF control, the use of dual implants, new neurotization surgeries for the reversal of denervation, new muscle transfer surgeries for high tetraplegia, and an improved forward dynamic model of the shoulder and elbow. During this contract period, all proposed neuroprostheses will come to fruition as clinically deployed and fully evaluated demonstrations.

Summary of activities during this reporting period

The following activities are described in this report:

- *Wireless data acquisition module for use with a neuroprosthesis.*
- *An implanted neuroprosthesis for functional electrical stimulation and myoelectric recording*
- *Simulated neuroprosthesis state selection and hand position control using myoelectric signals from a wrist flexor and extensor.*
- *An integrated voluntary muscle and FES controller to restore elbow extension in spinal cord injury*

Wireless Data Acquisition Module for Use with a Neuroprosthesis

***Contract section**:* E.1.a.v Sensory feedback of contact and grasp force

Abstract

The originally proposed plan of developing a thumbnail-mounted contact sensor that is connected to a small wireless transmitter has been altered so that now a general wireless data acquisition module is being developed. In addition to the thumbnail-mounted contact sensor, this general module could be utilized for other sensors used with a neuroprosthesis, such as the shoulder or wrist position transducer, finger-mounted joysticks, or remote on-off switches. Currently these sensors are connected to a controller via cables, which are cosmetically unappealing to the user and often get caught on wheelchairs, causing them to be damaged. Switch-activated transmitters mounted on walkers have been used previously in FES applications [1]. Recent advances in wireless technology have reduced the complexity and size of the wireless circuitry and have increased the likelihood that a small, low power, reliable wireless link could be assembled from commercially available components.

Methods

Efforts in the last two quarters have focused on developing the microcontroller-based RF communication software that will interface with the 916 MHz, low-power transceiver module from RF Monolithics (DR3000). The Microchip PIC16LF872 microcontroller was selected for this project for several reasons. It incorporates 5 channels of 10-bit A/D, has Flash memory to allow iterative programming, allows in-circuit serial programming and debugging, can operate at the 3.3V power level that the transceiver requires, and is available in a 28-pin SSOP package that measures 0.3" x 0.4" x 0.1".

The embedded software is being written using a C compiler that is optimized for the PIC microcontroller. The PIC-C compiler (CCS, Inc.) has device drivers and built-in functions for A/D sampling, serial communications, and other high-level operations that simplify the development process.

In most RF communication protocols, data and header information are combined in a packet to provide more efficient and accurate data transfer. The initial packet format being used in this project consists of a start symbol, a packet number, device ID numbers, and the sampled data value. The start symbol is a positive 100 μs pulse, indicating to the detection circuit that data is being sent. The packet number identifies the packet of data if acknowledgement or re-transmission is needed. The device ID numbers indicate which device is sending the message and for which device the message is intended.

Proper encoding of the data packet allows a symmetrical signal to be sent to the receiver, and is used by the noise rejection portion of the receiver circuit to improve data detection. DC-balanced encoding provides an equal number of 1's and 0's over a period of time. Manchester encoding is a popular method of DC-balanced encoding, in which each '1' is encoded as a '1-0' bit sequence, and each '0' is encoded as a '0-1' bit sequence (see Figure 1). This encoding method was used to encode the data packets.

Figure 1. Manchester encoding scheme (*courtesy of RF Monolithics, Inc.*).

Results

The software is being tested using a pair of demo boards from Microchip that include LEDs, switches, a potentiometer for varying an analog input, and connections for an RS232 serial link. Initially, the test circuits involved a wired-link between two microprocessors. This allowed a testing of the data sampling, packet creation, data encoding and decoding, and data extraction software routines without the complicating factors of RF noise. Once some timing issues were resolved, the transmitted data was received and decoded accurately.

The wired-link was then replaced with the transceiver modules. After modifying the software timing to accommodate for a slight delay from the RF transmission process, the data was transferred accurately. Figure 2 shows a sample packet of data recorded on a digital oscilloscope. This packet is packet #2, from device #1 to device #2, with a sampled data value of 78 out of a 0-255 bit range.

Next quarter

In the next quarter, several software features will be added. A CRC-error checking routine will be implemented, with a CRC value added to the end of each packet. If the packet is received without an error, an acknowledging packet will be sent back to the transmitting device. If an error occurs and the packet is not received properly, a "not acknowledged" message will be sent back to the originating device.

Bench tests will be performed on the wireless circuit to determine performance factors, such as the distance over which data can be transmitted successfully and the minimum data pulse size that can be detected (which will determine the maximum data transmission frequency).

Also in the next quarter, the hardware designs will be initiated for the circuit board that incorporates the miniature version of the microcontroller.

References

[1] Z. Matjacic, M. Munih, T. Bajd, A. Kralj, H. Benko, and P. Obreza, "Wireless control of functional electrical stimulation systems," *Artif Organs*, vol. 21, pp. 197-200, 1997.

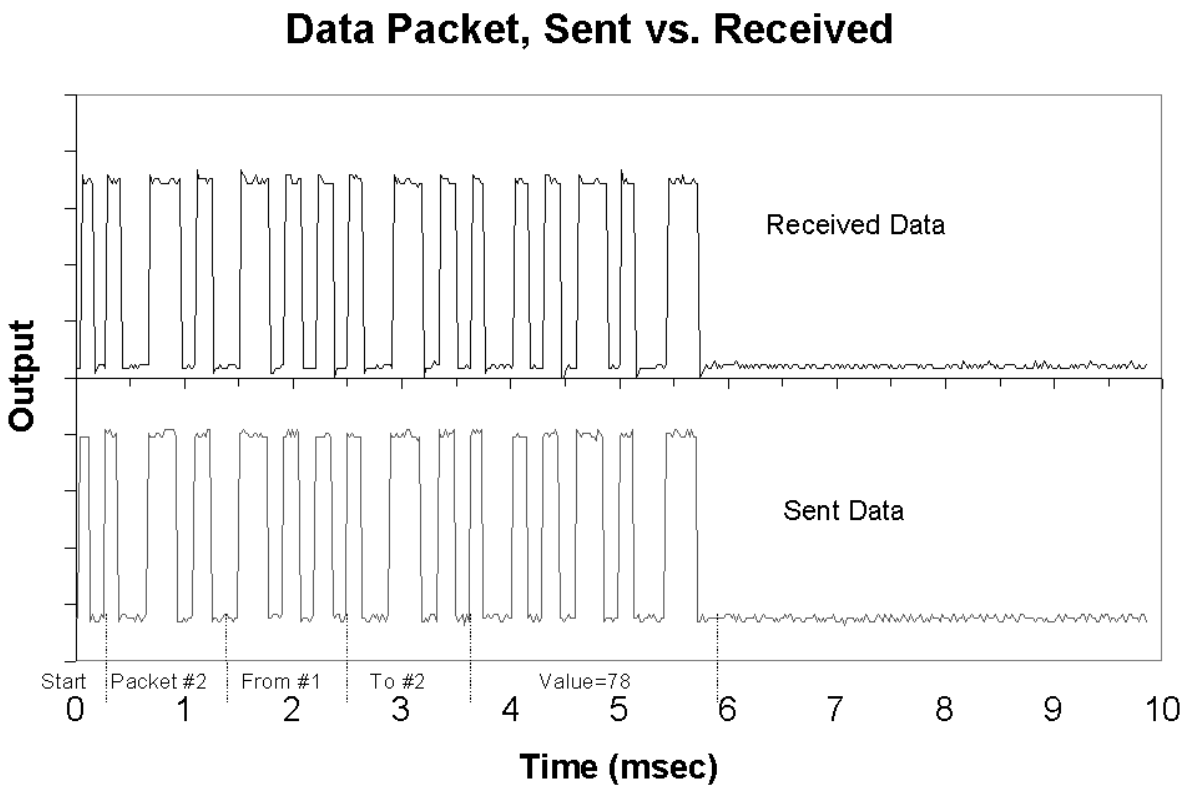

Figure 2. Comparison of a data packet sent and received via an RF link.

An Implanted Neuroprosthesis For Functional Electrical Stimulation And Myoelectric Recording

Contract section:
E.1.a.vi Implementation and evaluation of neuroprostheses for high tetraplegia

Introduction

The goal of this section of the project is to develop the hardware components necessary to implement advanced neuroprostheses for high tetraplegia. The key component of this effort is the development of an implanted stimulator/telemeter device that is capable of both electrical stimulation and myoelectric recording. Specifically, we are designing and fabricating an implanted neuroprosthesis that is capable of 12 channels of stimulation and has two channels of myoelectric signal (MES) recording. This device is being developed in a project funded outside of this contract. However, this device will be used in several projects within this contract and will be modified by contract work to incorporate the capability of nerve cuff stimulation. In this report, we present the evaluation of this device in a dog model to verify the ability to reject stimulus artifact while stimulating and recording.

Methods

The neuroprosthesis packaging was based on our first generation of implanted devices, and utilizes ASIC circuitry for flexibility. The implant package and electrodes are shown in Figure 3. The primary innovation in this generation is the recording of MES while stimulating. The stimulus artifact reduction was accomplished by reducing the gain on the MES inputs and integration amplifiers during stimulation, and pausing the recharge phase of the stimulus pulses while the MES is integrated for a period of approximately 30ms between pulses. Stimulation pulses are balanced charge, asymmetric, biphasic, constant current pulses which for these experiments were typically 20 mA with a pulse duration of 200 μsec and a frequency of 16 Hz. The neuroprosthesis was fabricated and bench tested in our design laboratories at Case Western Reserve University.

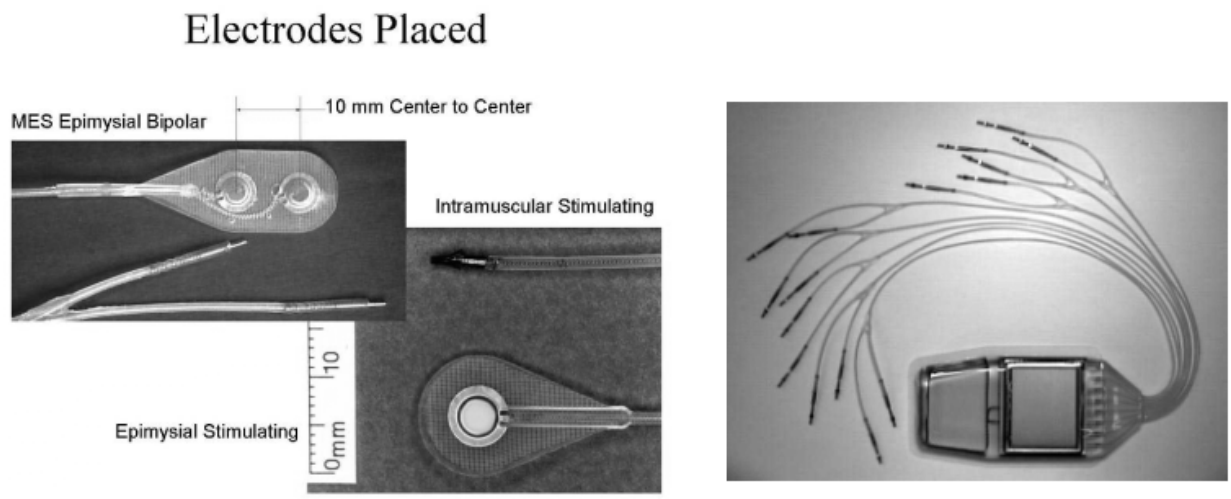

Figure 3. IST-12 implant package (on right) and stimulating and recording electrodes (left).

The neuroprosthesis was implanted in a dog in a pocket above the right shoulder. Stimulating electrodes were placed in the triceps and brachialis of the right leg and in the distal paw, shoulder, spine and ribcage, as shown in Figure 4. Bipolar epimysial MES recording electrodes, which were 4 mm diameter with 10 mm center-to-center spacing, were also placed on the triceps and brachialis, as shown in Figure 5 and Figure 6. Stimulation and recording from the implant were conducted both with the dog awake, to record normal activity, and sedated, using an injected signal. The MES was recorded during various combinations of stimulation. During the sedated experiments, a 100 Hz, square wave signal, gated at one Hz, was injected into the tissue using a pair of hypodermic needles in the right paw and the upper shoulder. The MES from the triceps and brachialis were also recorded externally using fine wire bipolar electrodes for comparison. A block diagram of the experiment is shown in Figure 7.

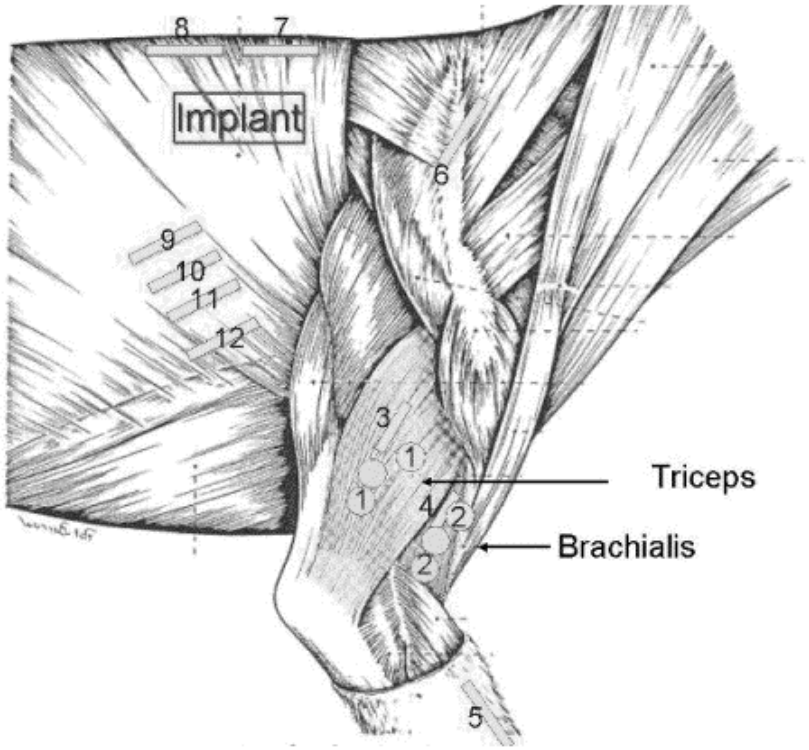

Figure 4. Location of stimulating and recording electrodes in the chronic dog implant.

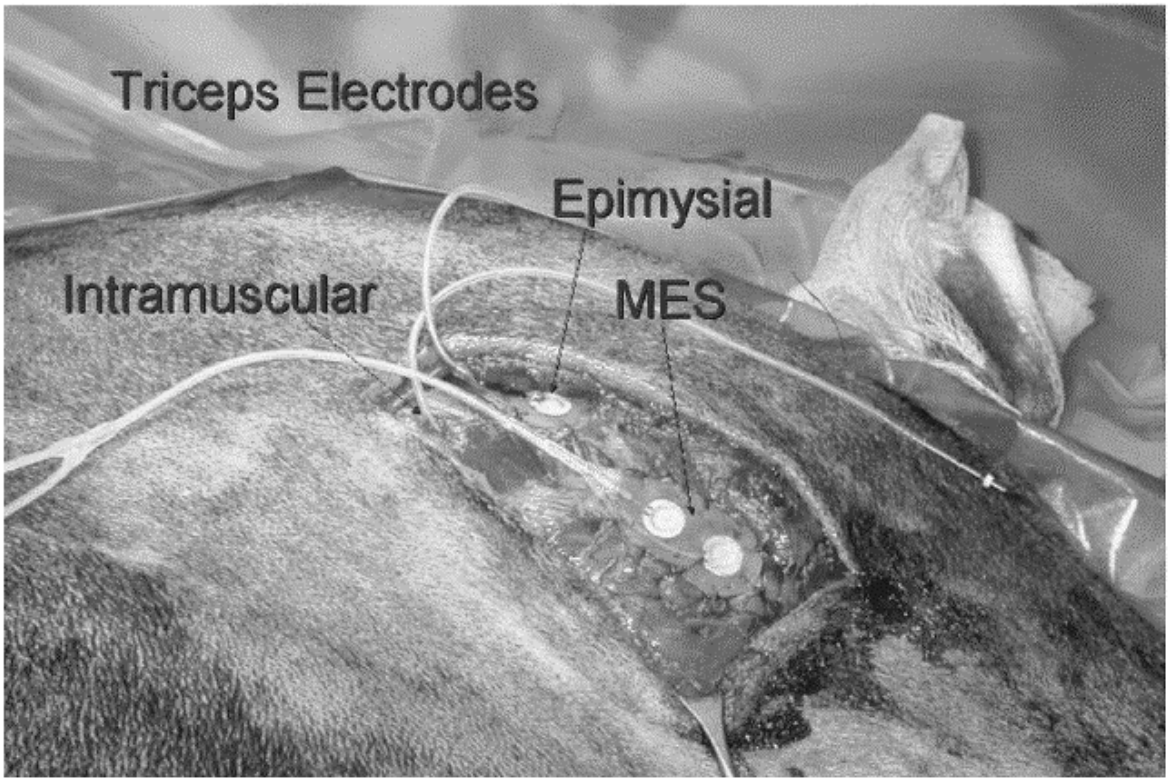

Figure 5. Triceps recording and stimulating electrodes.

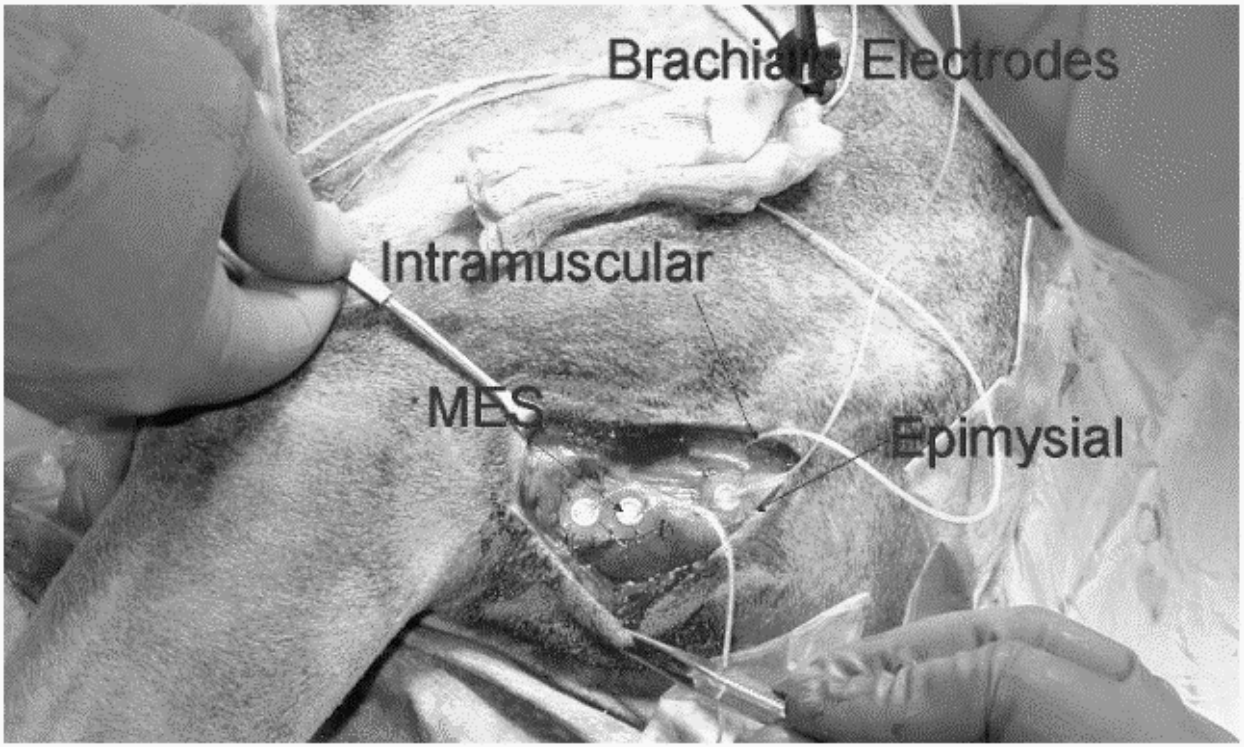

Figure 6. Brachialis recording and stimulating electrodes.

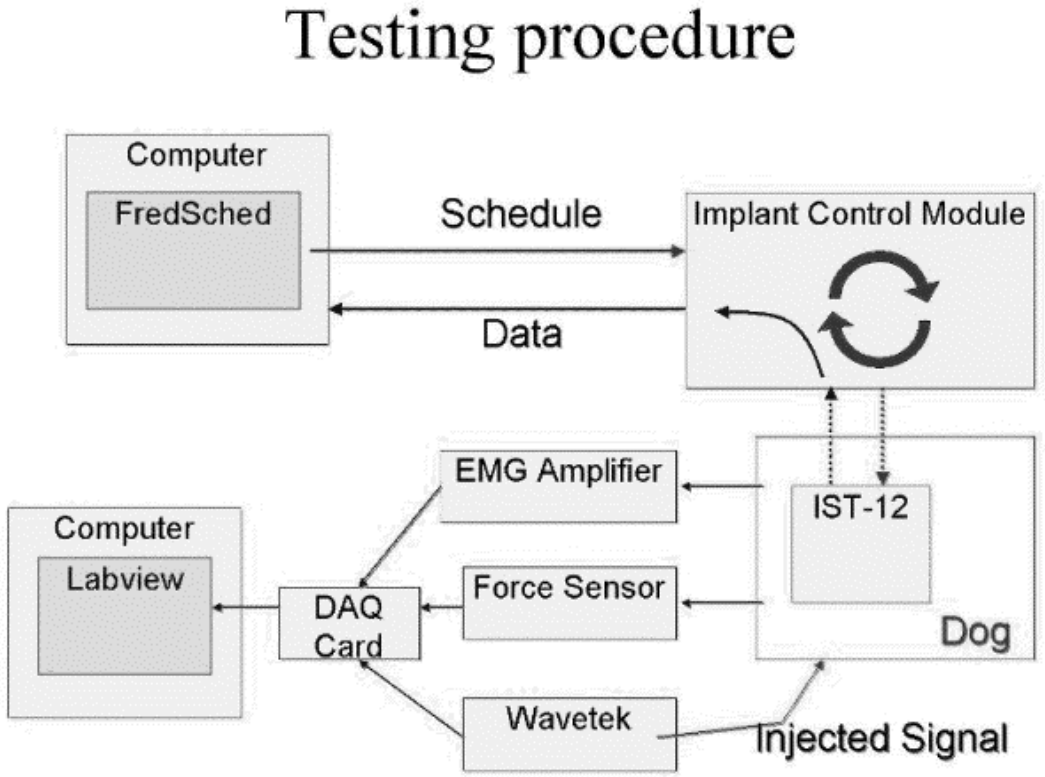

Figure 7. The MES activity from the muscles was recorded from both the implant and an external EMG amplifier in order to compare the signals.

Results

MES was successfully recorded from both muscles during awake movements, as shown in Figure 8. The stimulation artifact recorded from the MES electrodes, while stimulating from adjacent muscles, was less than 2% of the maximum recorded MES activity for any individual stimulating electrode and less than 3% for all seven stimulating electrodes fired before recording the MES. The results from these studies are shown in Figures 9 and 10, and summarized in Figure 11. The implant was able to record both integrated MES signal between pulses at up to 20 Hz and raw MES signal with no stimulation at a rate of 200 Hz.

Conclusion

The implanted neuroprosthesis performed as designed and provided a reliable, stable MES signal from adjacent muscles during stimulation. Pending successful completion of bench testing, this device is ready to proceed to human feasibility studies.

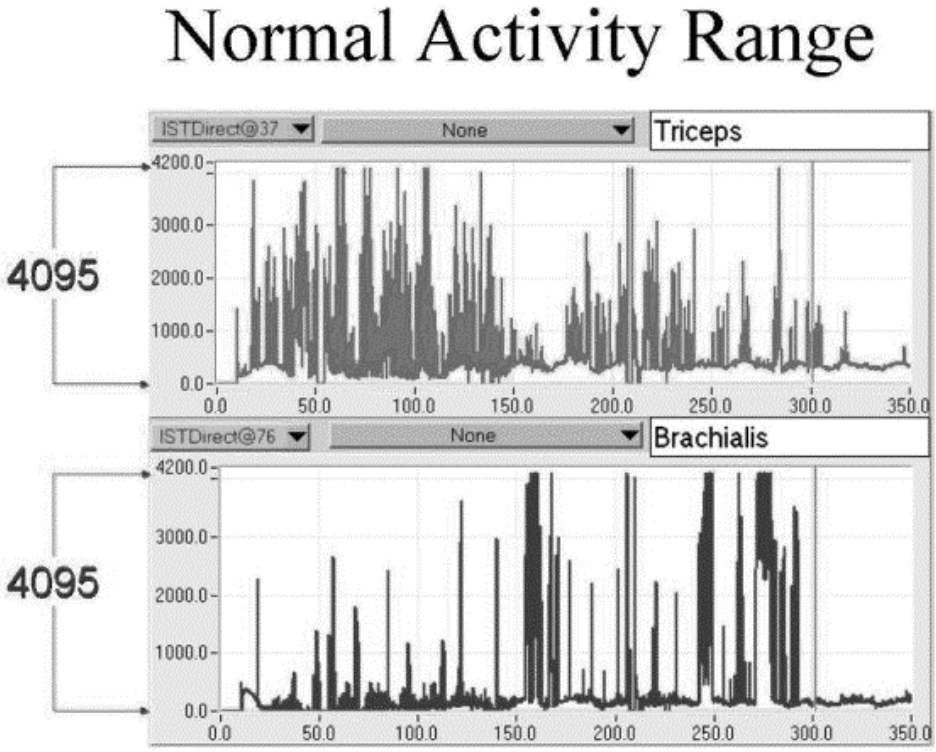

Figure 8. MES was recorded from both the Brachialis and Triceps while the dog was awake and walking about the room. This range was used for a baseline for comparison with artifact.

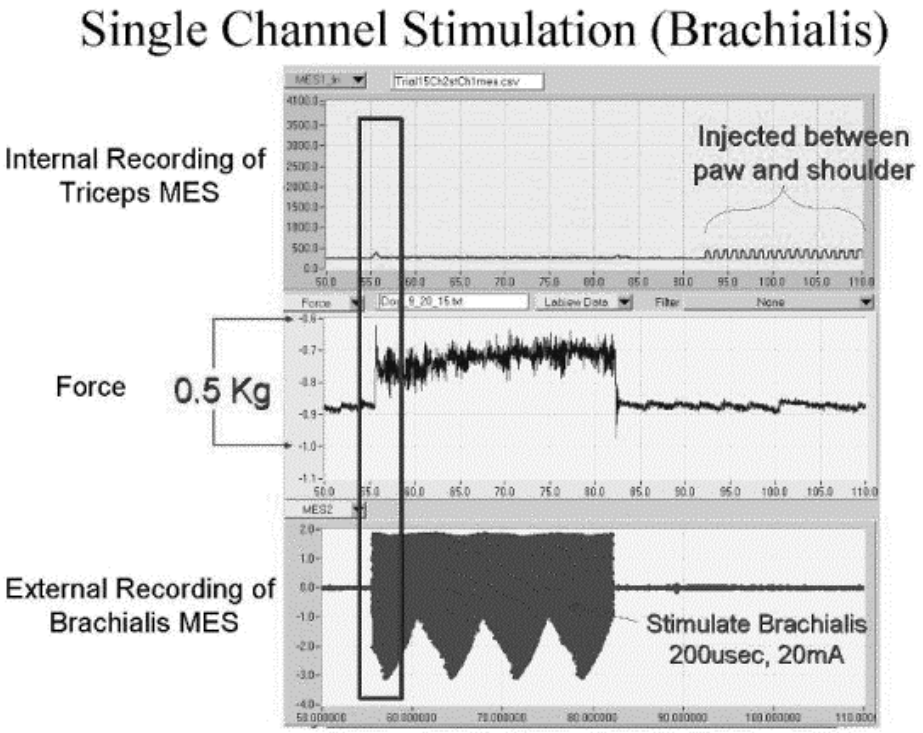

Figure 9. The external recording did not blank the artifact, while the internal recording blanked the artifact. The external force was measured as a gauge of the strength of the contractions. The section of the graph encircled in red is blown up to larger scale below.

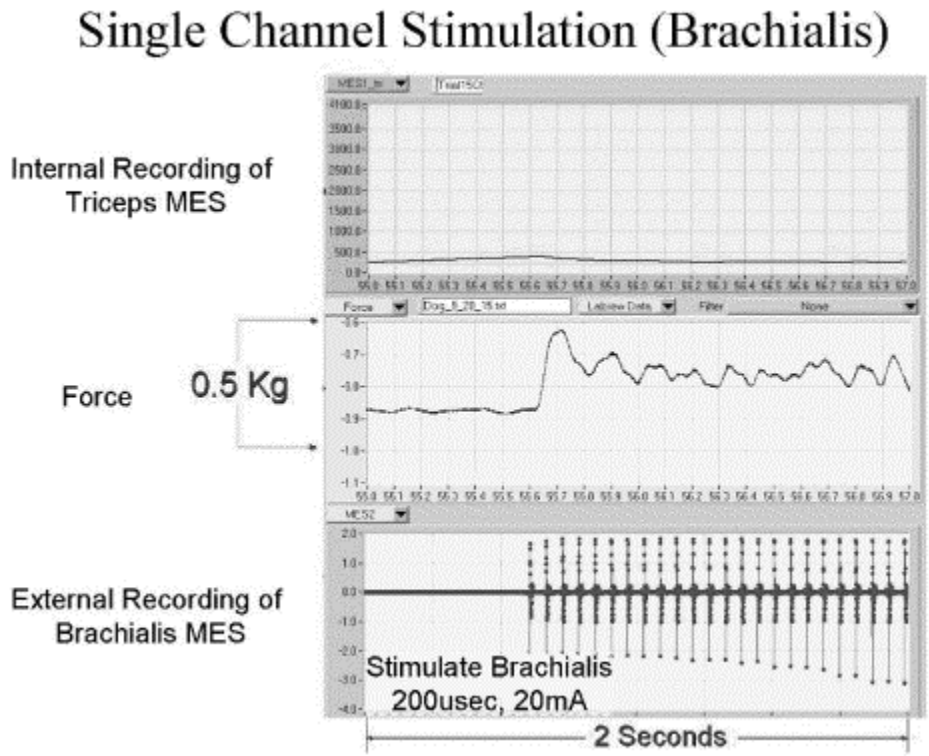

Figure 10. The stimulus pulses can be clearly seen on the external recording plot. The internal recording shows a small transient shift in the MES output.

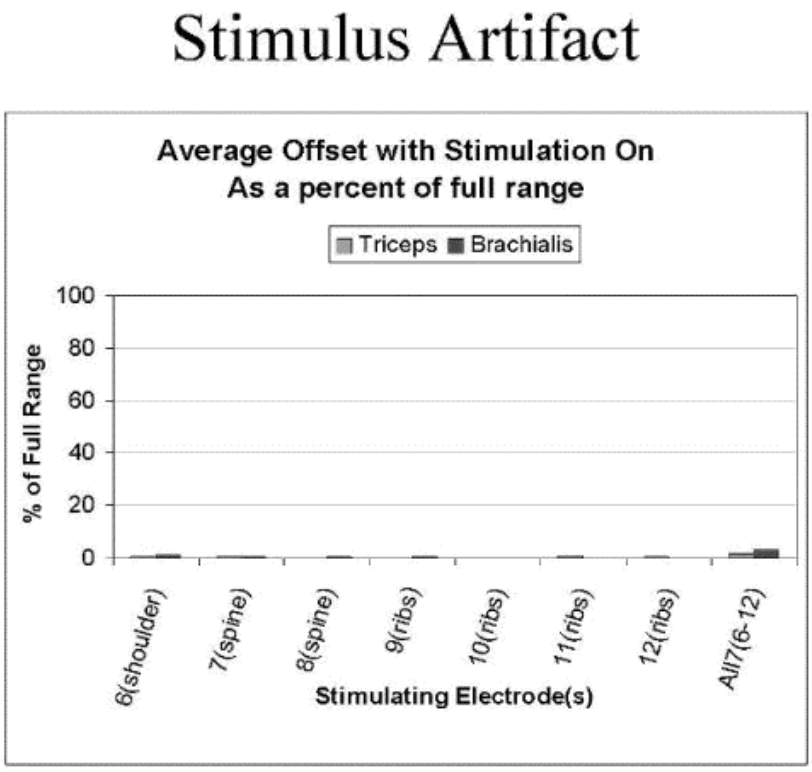

Figure 11. The stimulus artifact is shown here as a percentage of the full range during normal activity. Each channel was stimulated separately and all seven were also stimulated one after the other prior to recording the MES signal. The graph demonstrates an excellent level of artifact rejection.

Simulated Neuroprosthesis State Selection and Hand Position Control Using Myoelectric Signals from a Wrist Flexor and Extensor

Contract section: E.1.b Control of Grasp Release in Lower Level Tetraplegia

Abstract

The purpose of this research is to develop and evaluate an advanced neuroprosthesis to restore hand function in persons with OCu:5 and OCu:6 (International classification) spinal cord injuries. Through this work we will implement in human subjects a control methodology utilizing myoelectric signals (MES) from muscles synergistic to hand function to govern the activation of paralyzed, electrically stimulatable muscles of the forearm and hand. This work encompasses the following objectives:

1) Characterize the myoelectric signals recorded from a pair of muscles synergistic to hand function, demonstrating that the signals are suitable for neuroprosthesis control
2) Demonstrate the ability of subjects to use the proposed control algorithm to control a simulated neuroprosthesis
3) Implement myoelectric control of the hand grasp neuroprosthesis in subjects with C7 level spinal cord injury and evaluate hand performance

Methods

Work focusing on the first and second objectives continued this quarter. Data were analyzed that had been collected in experiments that were designed to investigate the ability of subjects to use myoelectric signals to perform simulated neuroprosthesis state selection and hand position control. In addition to the six able-bodied subjects reported on last quarter, a subject with C7 SCI (subject 7) participated in the study this quarter.

SCI Subject

Subject 7, a 50-year-old male, had grade 4 wrist extension and grade 3+ wrist flexion on the side that was tested (left). Only trace wrist flexion was present in the contralateral arm. Prior to these experiments, he was evaluated for FES intervention, and it was found that none of the finger or thumb muscles responded to electrical stimulation, suggesting denervation of these muscles. Time did not permit implantation of intramuscular electrodes for MES recording, because this subject was visiting our laboratory for a general evaluation for FES intervention. Therefore, we used surface electrodes to record from the wrist extensor and flexor.

Control Algorithm Design

Myoelectric signals (MES) from the extensor carpi radialis brevis (ECR) and flexor carpi radialis (FCR) were recorded during trials in which the subject was instructed to either relax the wrist muscles, flex the wrist, or extend the wrist. A ECR vs. FCR plot of the data revealed regions of the plot (MES-space) corresponding to wrist flexion, extension, and rest. Boundaries that define these regions were established and used to map the specific regions of MES-space (extension, flexion, and rest) to corresponding neuroprosthesis states (hand closing, hand opening, and hold). Subject 3 was unable to participate in the following two tests because the electrode wires fractured, perhaps as a consequence of rock-climbing the day in which the electrodes were implanted.

State Selection Simulation

The purpose of this test was to evaluate the ability of the subject to move a cursor into specific target regions shown on the computer screen (Figure 12). Successful positioning of the

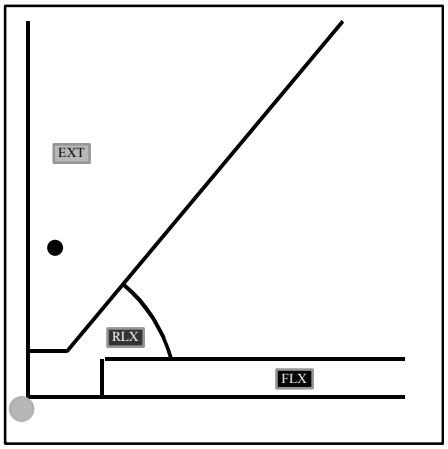

Figure 12. On-screen display during State Selection Test. Subject must move cursor into target region.

cursor into the target region corresponds to successfully selecting the neuroprosthesis state to which the region maps. The subject could move the cursor by flexing, extending, or relaxing the wrist muscles. The subject was cued to position the cursor in a region by a light that would appear in the target region. The subject had four seconds to position the cursor in the target region and keep it there until the target region changed. The target region cycled from Hold to Close to Hold to Open ten times. The subject was instructed to maintain a specific arm and forearm posture during this test. The test was repeated varying the arm (in front of the body vs. reaching) and forearm position (neutral vs. prone) as well as with and without a two-pound weight strapped to the hand to simulate wrist torque that may be expected during stimulation of finger flexors.

The value of this test is that it allows identification of errors that may be made in the process of selecting a desired state. This information is important for making modifications to the control algorithm that would reduce the likelihood of errors in neuroprosthesis state selection.

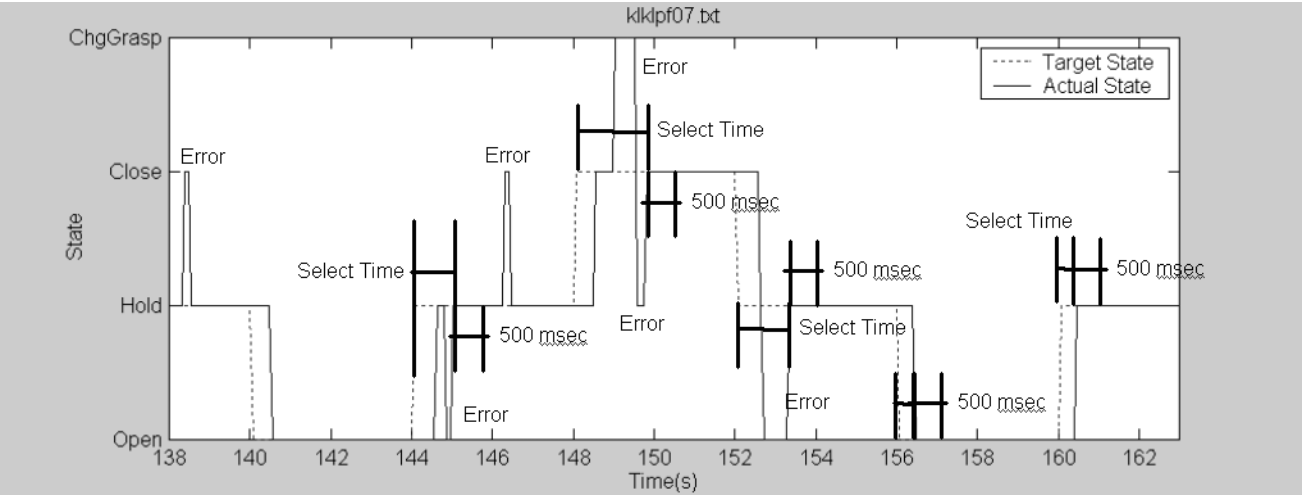

Figure 13. Sample of data from State Selection Test showing outcome measures explained in the text.

The performance measures on this test include the rate of successful state selection, average time to select the target state, the number and incidence of error, and the average duration of an error (Figure 13). A successful state selection was defined as positioning the cursor in the target region for 500 consecutive milliseconds. The time to select the target state was the time elapsed from commencement of the target cue to the beginning of the consecutive 500 msec defining successful selection. An error was defined as positioning the cursor in a non-target region, but did not include the expected delay of moving the cursor from the region it was in prior to the target change. The duration of an error was the amount of time the cursor was located in a non-target region.

Hand Position Control Simulation

The purpose of this test was to evaluate the ability of the subject to control the degree of opening and closing of an on-screen Pacman-like figure representing the hand (Figure 14). A target hand position was presented on the figure and the subject had eight seconds to match the target position by flexing and relaxing or extending and relaxing the wrist. When the position was within +/- 5 degrees of the target position, an indicator light appeared. The subject was instructed to correct overshoots or undershoots of the target position if necessary. The target

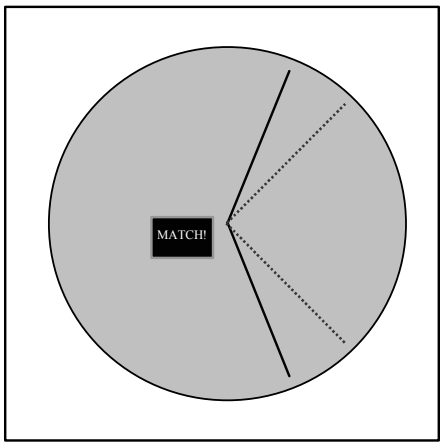

Figure 14. On-screen display during Position Matching Test. Subject open or close the "Pac-man" to match the target position.

position cycled from 25% fully closed to 50% to 75% ten times. As in the State Selection Test, this test was also performed at the different arm and forearm postures and hand loading conditions.

This test more closely simulates what the subject will be doing during actual use of the hand grasp neuroprosthesis. They will see their hand and will want to open or close it a certain amount in order to grasp or release an object. Performance on this test will provide a closer approximation of the degree of hand control that might be expected in actual use of their own hand under myoelectric control.

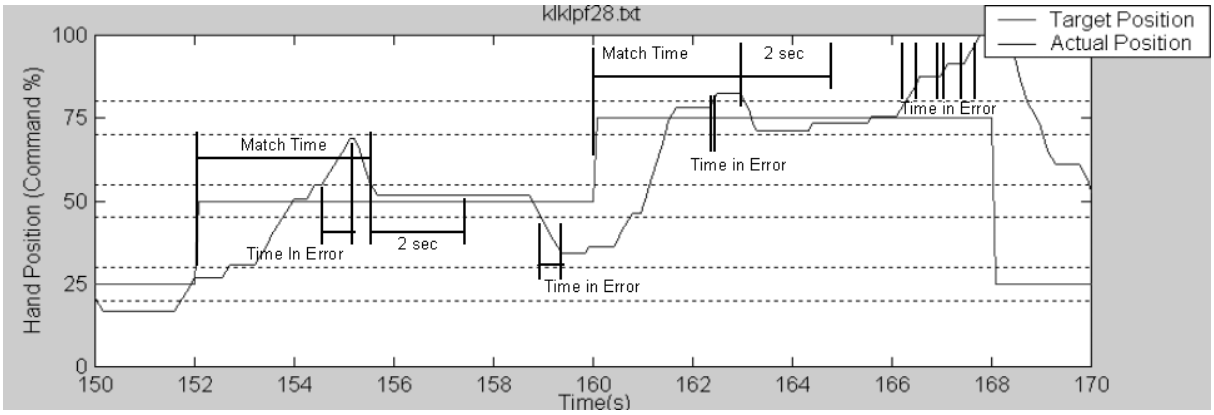

Figure 15. Sample of data from Position Matching Test showing outcome measures explained in the text.

The performance measures on the position matching test include the rate of successful position matching, the average time to match the target position, and the time spent in error (Figure 15). A target position was successfully matched if the actual position (expressed as a percentage of full closure) remained within +/- 5% of the target position for two consecutive seconds. The time to match the target position was the time elapsed from the start of the target cue to the beginning of the consecutive two seconds defining successful position matching. An error in this test was defined as occurring when the subject-controlled hand position was moving away from the target position.

Results

Control Algorithms

The MES data and boundaries for the six able-bodied subjects were shown in last quarter's report. The data from the C7 SCI subject is shown in Figure 16. The data collected during wrist flexion and extension occupy distinct regions of the MES space.

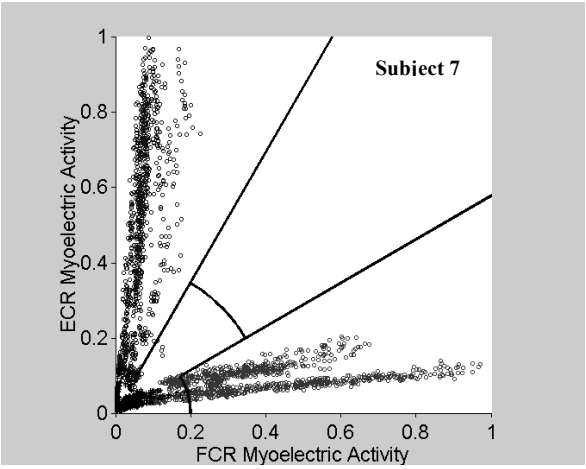

Figure 16. Data from SCI subject showing distinct regions corresponding to wrist flexion and extension.

State Selection Test

The pooled results for each tested subject are shown in Figure 17. Every subject but one (subject 4) selected the desired neuroprosthesis state (positioned the cursor in the target region) with a success rate of 100% of the 320 presented targets. Subject 4 failed to position the cursor in the target region once, giving a success rate of 99.7%. These high success rates indicate high proficiency in selecting each of the neuroprosthesis states. However, it doesn't provide information as to the errors made or difficulty in achieving the successful selection of a state.

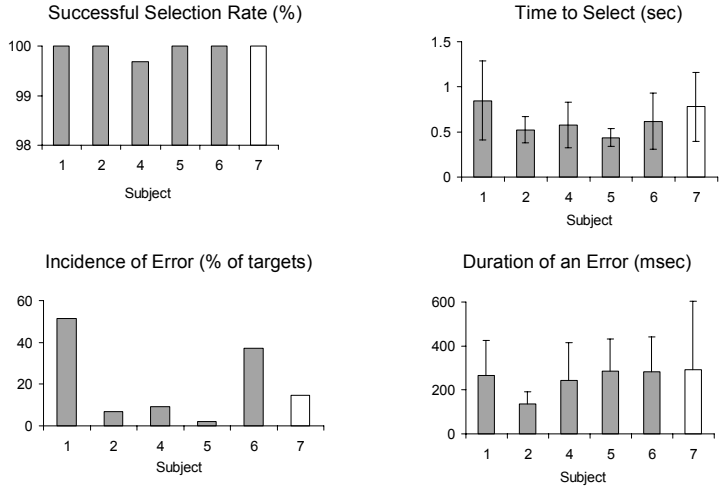

Figure 17. Performance on State Selection Test. All subjects could select desired state with high proficiency. Subjects 1 and 6 had high incidence of errors.

The average time to successfully select the state ranged from 435 to 850 msec. A delay of up to about 600 msec is expected due to signal processing and reaction time. Therefore, selection times greater than 600 msec are indicative of either excessively long reaction time, or the occurrence of errors prior to successful selection of the state.

The incidence of error is the percentage of the number of target presentations (320) during which one or more errors were made. This percentage ranged from 2% to 52%. Subjects 1 and 6 had the highest incidence of error. The high rate of error in these two subjects was due to bursts of flexor activity that occurred when the wrist was extended (Figure 18). These bursts at the beginning and end of wrist extension caused the cursor to enter into unintended regions of MES space during the transition from Hold to Close and from Close to Hold. This muscle activity, presumably a stretch reflex response, did not commonly occur in the other subjects.

The average duration of an error was less than 300 msec for all subjects. The duration of an error corresponds to the magnitude of unintended change in hand position. A 300-msec error would correspond to a change in hand position of 8 to 15% assuming a speed of hand opening and closing set between 25% and 50% per second.

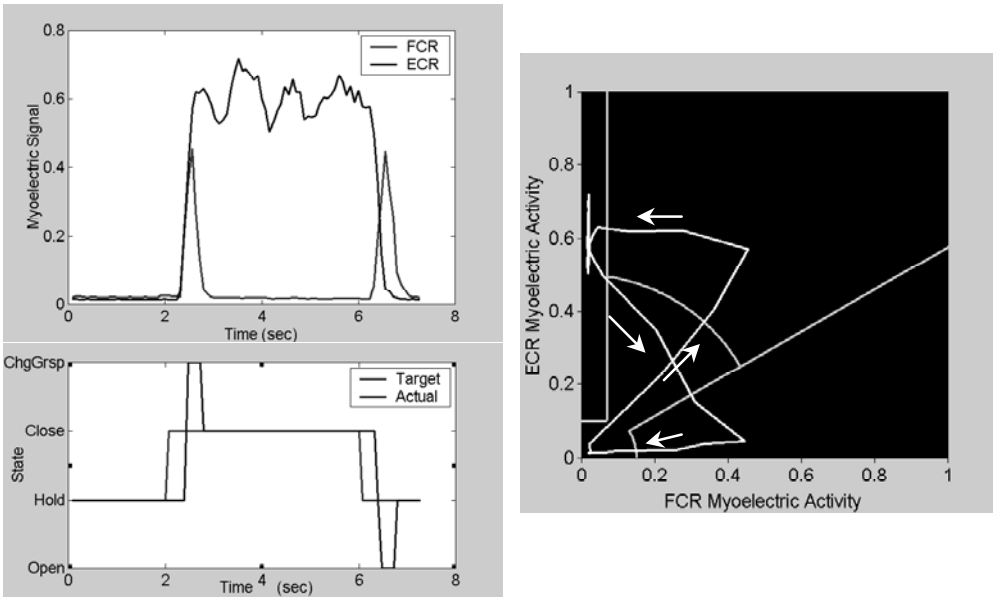

Figure 18. Example of a common error made by subjects 1 and 6 caused by stretch reflex burst of activity in wrist flexor during wrist extension.

Position Matching Test

The pooled results for each tested subject are shown in Figure 19. Every subject was able to match hand positions with a success rate greater than 85%. Four of the six subjects had a success rate greater than 98%. These high success rates indicate proficiency in controlling the position of the simulated hand.

The average time to successfully match the target position ranged from 1.7 to 3.2 seconds. Besides signal processing, reaction time, and time spent overshooting or undershooting the target, this time also depends on the position change required and the speed setting of opening and closing. The lowest possible average match time is approximately 1.3 sec (assuming a reaction time of 300 msec). Match times greater than 2 seconds may be indicative of slow reaction times, undershooting the target position, or overshooting the target (errors).

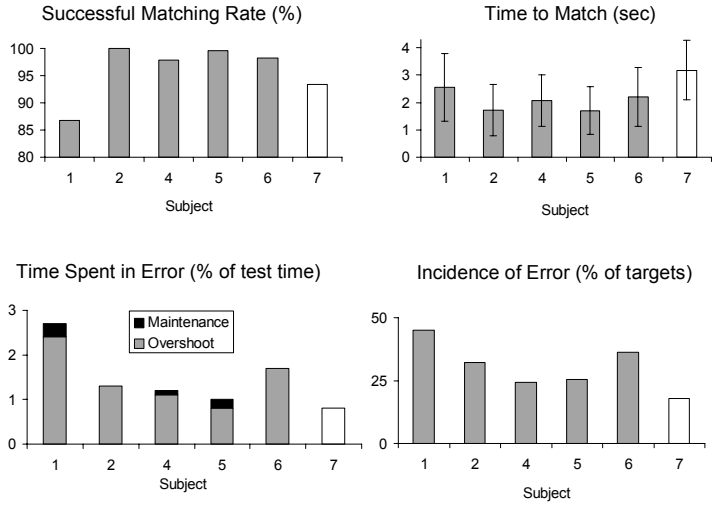

Figure 19. Performance on Position Matching Test. All subjects could match target hand position with high proficiency.

The accumulated time spent in error, expressed as a percentage of the total test time, ranged from 0.8% to 2.7%. Another way of expressing the error rate is as a percentage of the number of target presentations (240) during which one or more errors were made. This incidence of error ranged from 18% to 45%.

Examination of errors on a subject-by-subject basis is required to make modifications to the control algorithm that would reduce the error rate. Methods for classifying errors according to their severity (determined by considering the possible consequences of an error) are being developed.

Conclusions

These results satisfy our second objective. They demonstrate that subjects can use myoelectric signals from wrist muscles to control on-screen displays that simulate selection of neuroprosthesis states and control of hand position. Subjects have been found to make significantly more errors during transitions between desired states than during attempts to maintain a desired state. Also subjects have more difficulty in achieving a desired hand position without overshoot than they have in maintaining the hand position once they have achieved it. The nature of errors made in selecting neuroprosthesis states and in controlling hand position can be identified, and this information can be used to make modifications to the control algorithm.

Next Quarter

Individuals with C7 SCI will be recruited to participate in the protocol. The experiments described in this and the previous progress reports will be done with two more SCI subjects. In addition, preparations for percutaneous implementation and testing of myoelectric control of FES will be completed.

An Integrated Voluntary Muscle and FES Controller to Restore Elbow Extension in Spinal Cord Injury

Contract section: E.2.a.ii.4.1 EMG-based shoulder and elbow controller

Abstract

The objective of this research is to develop and assess a synergistic control scheme employing the remaining voluntary elbow flexor and shoulder electromyograms (EMG) in individuals with C5/C6 spinal cord injury (SCI) to control elbow extension using functional electrical stimulation (FES) of the triceps. The controller should detect subject arm intention and provide the required elbow extension. We hypothesize that the remaining voluntarily-controlled upper extremity muscles of a C5/C6 SCI subject produce a recognizable pattern of EMG signals indicative of the level of triceps stimulation needed for the desired position and endpoint force of the arm.

Methods

The controller should allow subjects to generate and control endpoint force vectors that are unachievable without triceps stimulation. To accomplish this, the network must be trained with endpoint force vectors outside of the subject's voluntary range. This requires triceps stimulation. Additionally, once trained, the network will operate during triceps

stimulation. A catch-22 exists. We want to train an artificial neural network (ANN) to output triceps stimulation, but need to train that ANN with EMG collected during the correct level of triceps stimulation. The ANN will be trained with EMG collected as a subject generates goal isometric force vectors. We need a good stimulation level estimate for each goal vector to break out of the catch-22.

A biomechanical model is capable of estimating the force and moment contributions of individual proximal arm muscles based on kinematic and kinetic inputs. Specifically, if we specify external forces and arm geometry, the model will predict the joint moment needed to be produced by the triceps. This model uses a finite element method to determine muscle activations for given inputs, including the orientation of the arm and external forces acting on the hand. The optimization criterion of this model minimizes the squared sum of the muscle stresses (muscle force/physiological cross sectional area of the muscle). This model was chosen since it allows users to specify voluntarily controlled muscles and their strength. We tailored the model for each subject to give us subject specific outputs based on their specific remaining voluntary muscle set.

We ran simulations using the model to find the elbow extension moment required by the triceps for a specific subject for each goal isometric endpoint force vector (location, direction, and magnitude). We accomplished this by removing paralyzed muscles from the model, reducing the force capability of weak muscles, and keeping normal the muscles still under strong voluntary control. However, we assumed a near normal triceps since FES can restore its ability to generate forces. By defining the triceps muscle as normal in the model, we obtained the triceps elbow extension moment needed to achieve the desired endpoint force output. The elbow extension moment needed will be a function of the subject's voluntary set of muscles and arm kinematics. Therefore, we defined particular kinematics of the arm for each location that will be tested. The biomechanical model yielded a reasonable estimate of the triceps extension moment that should be applied for a given goal.

The biomechanical model yielded elbow extension moments required by the triceps. However, we needed to know the correct level of triceps stimulation to apply. For each subject, we experimentally measured elbow moment as a function of stimulus level (recruitment curve). The elbow extension moment yielded by the model was converted to triceps stimulation using the inverse of the recruitment curve. Recruitment curves for elbow extension versus triceps stimulation level were collected using an elbow moment transducer. The stimulation was increased in discrete levels by gradually increasing the stimulation pulse width. Data was collected for various angles and arm orientations that match anticipated data collection positions. The inverse recruitment curves were created by fitting a polynomial to scatter plots of triceps stimulation versus elbow extension moment.

Results

The biomechanical model produced the moment required by the triceps to achieve endpoint force vectors of the desired magnitude and direction. Shown below are the results for the set of muscles remaining under voluntary control in one subject as well as his inverse recruitment curve (Figure 20 and 21).

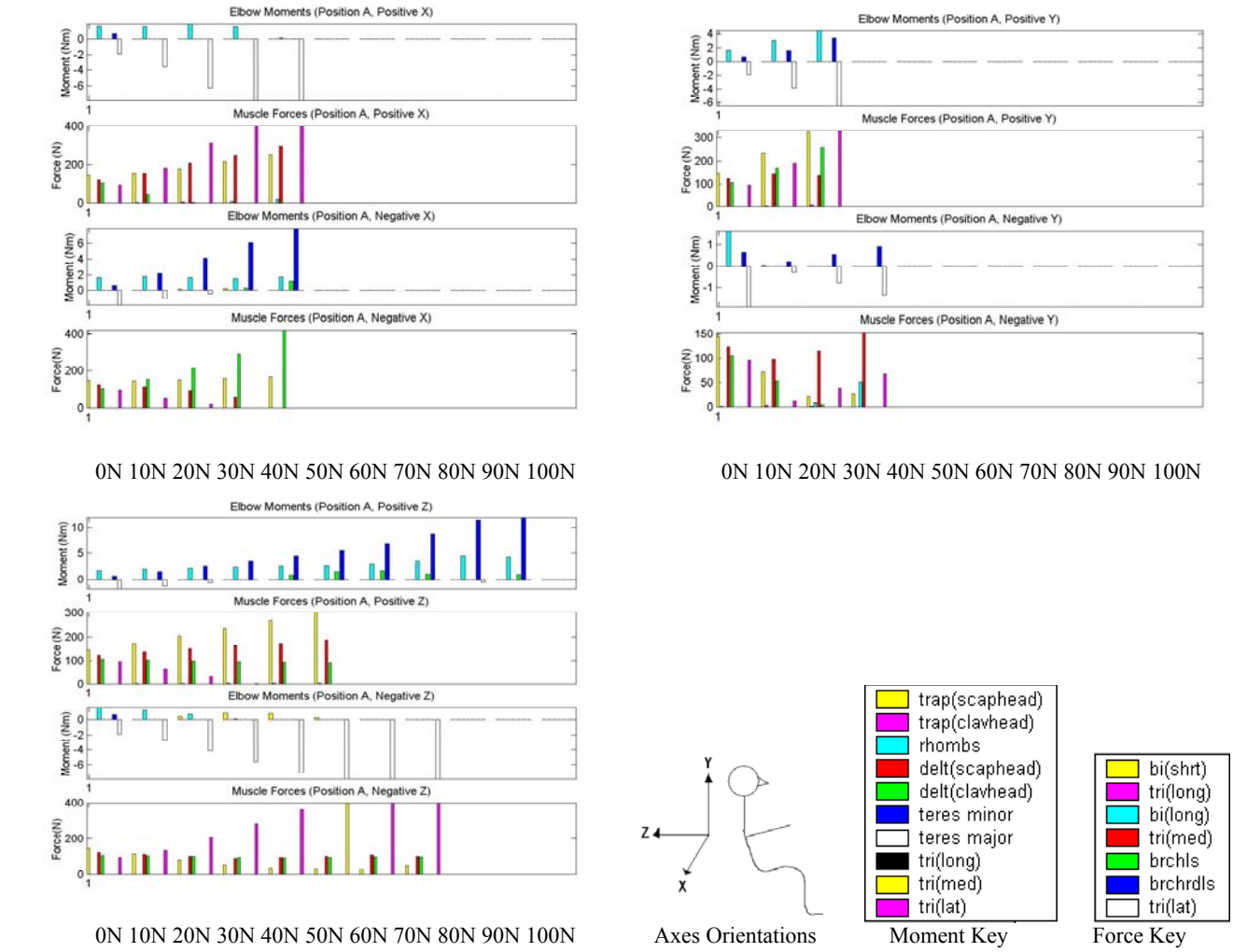

Figure 20. The moments about the elbow and forces produced by specific proximal arm and shoulder muscles are plotted as a function of increasing force along a specific axis and direction. The orientations of the axes are shown as well as a muscle force and moment key.

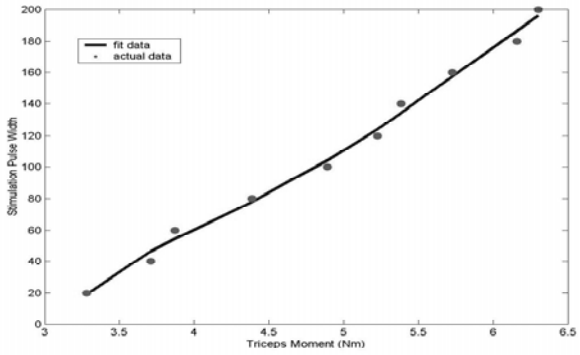

Figure 21. The inverse recruitment curve was calculated by plotting elbow moment versus triceps stimulation pulse width.

The model predicted that the medial and lateral head of the triceps are needed to produce an elbow extension moment when forces are produced along three of the six directions simulated. An elbow extension moment is not required for forces in the other directions and hence neither is triceps stimulation. For the left arm, an elbow extension moment from triceps is required to produce forces in the negative x, negative z, and positive y directions. The elbow extension moment required increases as a function of force magnitude along the axis. Force magnitudes that show no muscle activation in the plots illustrate locations that cannot be achieved by a subject with this remaining voluntary muscle set regardless of the amount of triceps activation provided. Plugging the predicted moments into the polynomial fit of the inverse recruitment curve has allowed us to predict triceps stimulation levels that will be required for SCI subjects to generate isometric force vectors with different directions and magnitudes in space.

Next Quarter

Surface EMG will be collected from subjects' voluntary elbow flexor and shoulder muscles while they generate isometric endpoint force vectors at a variety of arm postures. Stimulation will be delivered to the triceps during the experiment as predicted by the model and inverse recruitment curves. Subjects will wear a cast to stabilize their wrist, with the cast attached to a 6-axis force and moment transducer. A visual display will provide magnitude and direction feedback of the goal and generated force vectors. Data will be collected from subjects during two separate sessions. Five different locations will be tested in each session, with one overlapping location (A), for a total of nine locations tested (Figure 22). During each session there will be a total of sixty-five trials. At each of the five locations, subjects will generate thirteen goal vectors: a net zero force vector and two magnitudes of force in each of six directions: +x, -x, +y, -y, +z, and -z. Magnitude and direction will be randomized. Location order will be randomized, however, all trials will be completed at one location before moving to another to reduce session time and minimize subject discomfort.

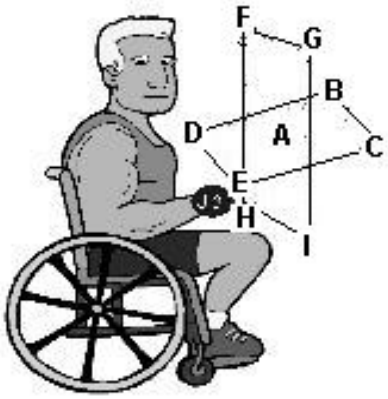

Figure 22. Data collection will be completed as subjects generate isometric endpoint force vectors at nine locations in space.